Available online at www.sciencedirect.com
SCIENCE DIRECT®
PERGAMON
International Journal of Heat and Mass Transfer 46 (2003) 4145–4155
International Journal of HEAT and MASS TRANSFER
www.elsevier.com/locate/ijhmt

Study of free-convective onset on a horizontal wire using speckle pattern interferometry

D. Ambrosini [a,*], D. Paoletti [a], G. Schirripa Spagnolo [b]

[a] INFM, Dipartimento di Energetica, Università di L'Aquila, Loc. Monteluco di Roio, I-67040 Roio Poggio (AQ), Italy
[b] Dipartimento di Ingegneria Elettronica, Università degli Studi di Roma Tre, I-00146 Roma, Italy

Received 2 January 2003; received in revised form 13 May 2003

Abstract

The onset and development of heat convection from a suddenly heated thin horizontal wire in air has been studied experimentally by an optical technique, named dynamic electronic speckle pattern interferometry, which allows the acquisition of qualitative and quantitative data. Attention is focused in providing temperature field visualizations and data about the temporal behavior. The heat-rate-based Rayleigh number, Ra^*, ranges from 0.069 to 0.67, a region of parameters poorly covered by previous investigations. Experimental results are compared with previous data. The extent, at which existing correlations can be used for wires of 0.2 and 0.4 mm in diameter, is outlined. A new correlation is proposed.

Keywords: Transient natural convection; Horizontal cylinder; Electronic speckle pattern interferometry

1. Introduction

Natural convection is important in many engineering applications. It plays either a dominant role or a role that significantly affects transport processes. Furthermore, convection heat transfer, which historically grew out of power plant technologies and aircraft, has now to face additional challenges in the areas of energy, ecology and cooling of electronics components [1]. As a result, free convection has been receiving increasing attention and is extensively reviewed [2–5]. In particular, because of its engineering interest natural convection from horizontal circular cylinders and from line heat sources has been studied, both numerically and experimentally [6–12].

Transient behavior is very important itself and in many related engineering situations. In literature, great attention has been given to transient free convection above plates [13,14], but only a comparatively smaller amount of data are available about horizontal cylinders [15–17].

If suddenly heated by a step change in heat rate, the heat transfer in a fluid surrounding a horizontal cylinder or wire, is initially by pure conduction and is then followed by a transient convective regime. The problem of pure conduction from a small circular cylinder, subject to constant heating at time $t = 0$ and dissipating in an infinite medium, has been analytically described by Blackwell [18]. Carslaw and Jaeger [19] presented the initial temperature response, in terms of Bessel functions, for a perfectly conducting cylinder with finite heat capacity. A simple approximation to the Carslaw and Jaeger's solution was given by Vest and Lawson [16].

Ostroumov [15] was the first to perform experimental work on the onset of convection near a suddenly heated horizontal wire. He used an optical technique to visualize the temperature pattern and a resistance bridge to measure the temperature of the wire. His flow visualization showed the initial conductive behavior, characterized by isotherms in the form of concentric circles in

* Corresponding author. Tel.: +39-0862-434336; fax: +39-0862-434303.
E-mail address: dario@ing.univaq.it (D. Ambrosini).
URL: http://dau.ing.univaq.it/~laser

0017-9310/$ - see front matter © 2003 Published by Elsevier Ltd.
doi:10.1016/S0017-9310(03)00266-7

Nomenclature

c	specific heat of fluid (at constant pressure)
d	diameter of test cylinder
g	gravitational acceleration
Gr	Grashof number, $g\beta(T_w - T_\infty)\rho^2 d^3/\mu^2$
h	convective heat transfer coefficient, $q'/\pi d(T_w - T_\infty)$
I	light intensity, see Eq. (6)
I_o	intensity of the object light beam, see Eq. (6)
I_r	intensity of the reference light beam, see Eq. (6)
k	fluid thermal conductivity
n	refractive index of air
Nu	Nusselt number, hd/k
P	laser power
Pr	Prandtl number, $c\mu/k$
q'	wire linear heat rate
Ra	Rayleigh number, $Gr \cdot Pr$
Ra^*	modified Rayleigh number, $Ra \cdot Nu$
t	time
t^*	time at which significant convection begins
T	temperature
x, y	coordinates centered on the cylinder axis

Greek symbols

α	thermal diffusivity of fluid, $k/\rho c$
β	coefficient of thermal expansion of fluid
ϑ	optical noise term
φ	optical phase
$\Delta\varphi$	optical phase variation, see Eq. (5)
λ	laser wavelength
μ	dynamic viscosity of fluid
ρ	density of fluid
τ	Fourier number, $4\alpha t/d^2$
τ_D	Fourier number at onset of convection ("delay time")

Subscripts

w	relative to the wire
∞	relative to the ambient (or undisturbed) conditions

the axial plane, and the existence of a delay between the beginning of constant heating and the development of observable convection. This delay is now usually [5] described through the Fourier number at the onset of significant convection, $\tau_D = 4\alpha t^*/d^2$, referred to as "time delay" or "limit of pure conduction" [17].

Ostroumov failed to understand the process clearly, however, as was noted afterwards [16,17], his experimental results can be combined to suggest a delay time of the form

$$\tau_D \sim (q')^{-0.6}. \tag{1}$$

Successively, Vest and Lawson [16] performed experimental investigations using a Mach–Zehnder interferometer. Their observations confirmed the existence of a pure conduction initial stage (isotherms as concentric circles) followed by a transient convective stage in which the isotherms became asymmetrical until they formed the familiar mushroom-shaped plume and afterwards reached the steady state. Vest and Lawson proposed a simple theory to explain the transient behavior as the result of thermal instability. By supposing similarity with the Bénard problem of a fluid heated from below, they assumed the existence of a critical Rayleigh number, which defined the breakdown of pure conduction. Using an approximate temperature profile and a critical Rayleigh number of 1100 (as in the Bénard problem with rigid lower and free upper boundaries [20]) they derived an expression for the delay time as a function of the linear heat rate. Their expression was then rewritten by Parsons and Mulligan in terms of delay time, using a modified Rayleigh number Ra^* based on the heating rate and defined as $Ra \cdot Nu$, in the following manner [17]

$$\tau_D = 80.2(Ra^*)^{-2/3}, \tag{2}$$

which is now generally accepted as the standard correlation for the delay time [5].

Parsons and Mulligan [17] determined the response of suddenly heated horizontal wires using a resistance bridge, providing data both for the transient and for the steady-state free convection. The accordance between their data and Vest and Lawson's results is good. In fact, Parsons and Mulligan's best fit regression line

$$\tau_D = 80.7(Ra^*)^{-0.64} \tag{3}$$

is very close to Eq. (2). Parsons and Mulligan also proposed a regression line, only for the air data, as follows

$$\tau_D = 136(Ra^*)^{-0.58}. \tag{4}$$

In this case the accuracy of the line is better.

The transition from pure conduction to steady-state convection can occur by conduction heat transfer at τ_D greater than the steady-state value, in this case Nu falls monotonically; otherwise by an overshoot in the wall temperature. The value of the critical overshoot Rayleigh number, above which no overshoot occurs, can be derived by the graph proposed by Parsons and Mulligan [17].

The first two experimental works were primarily optical. However, Ostroumov's pioneering paper gave some inconsistent data. Vest and Lawson's paper is a short note and only flow visualization in water is presented. On the other hand, Parsons and Mulligan provided a great amount of data but no visualizations.

Despite the growing importance of sophisticated numerical methods experimental quantitative and qualitative observations are still necessary to develop a more complete phenomenological theory and to compare the obtained data to previous analytical and numerical investigations [21,22]. However, very few experimental investigations are available in literature about transient convection from horizontal wires, especially for full-field measurements.

In this paper we report the results of an experimental investigation on the onset of convection from horizontal cylinders in air. Attention is focused on the temporal behavior. Our aim is to provide more qualitative and quantitative data through an instrumentation able to study transient processes at a relatively low cost. To achieve this objective, we performed intensive flow visualizations to investigate convection onset and the transition mechanism from onset to steady state. Then time delay was determined, identifying the onset of convection by the same criteria used by Vest and Lawson [16] and the results were compared to other studies.

Visualization experiments were performed using an optical method based on the electronic speckle pattern interferometry (ESPI). This technique, briefly described in Section 2, provides interferometric-like images, that allow an all-digital temperature field mapping. Futhermore, the system makes possible full-field, non-contact, time-sequence investigations of heat transfer processes. Experimental results are given in Section 3.

2. Experimental apparatus and procedure

Due to their features, a great variety of optical techniques [23–25] have been used to investigate thermal layers. As they are non-contact, optical methods do not disturb the temperature field. There are no inertial errors and full-field temperature data of rapidly changing processes can be provided. The most popular optical methods, among heat and mass transfer practitioners, are interferometry [26], holographic interferometry [27], speckle photography [28] and Schlieren [29]. Holographic interferometry, in particular, represents a preferable choice for flow visualization in electronics systems [30].

ESPI [31] is an interferometric technique, which is increasingly used in experimental mechanics and nondestructive testing. It has also been applied to some heat and mass transfer problems [32–35] such as, for example, isothermal diffusion in binary liquid mixtures [32,33] and steady state heat transfer from horizontal plates facing downward [34].

In this work, to study transient processes in free convection, we used a method based upon the ESPI technique. In transient events, the phenomena can probably be best understood by viewing video registrations of the flow evolution while more detailed information can successively be extracted from time sequences of images. Starting from these basic ideas, various refinements and developments have been used in the past years. In particular, Vest and Lawson [16] visualized temperature patterns around a thin wire by a Mach–Zehnder interferometer and then recorded the transient with a 16-mm movie camera at a speed of 32 or 64 frames/s.

The ESPI, often referred to as TV-holography, was developed in the early 1970s as a method of producing interferometric data electronically without using the traditional holographic recording technique. ESPI has been widely used for dynamic measurements [36] in vibration analysis; basic instrumentation involved the use of high-speed cameras and pulsed lasers. Here we used a method, based on standard ESPI system, capable of investigating transient events. Following Ahmadshahi et al. [37], we called this technique Dynamic-ESPI. Ahmadshahi et al. proposed an ESPI implementation for vibration measurements in which speckle patterns are recorded on a photographic emulsion using a high-speed camera, subsequently the negatives are digitized and digitally elaborated. As will be more clear in the following, our technique can be considered as a simplified and improved all-digital version of the arrangements described in [16,37].

A sketch of the present experimental setup is shown in Fig. 1. Here we give a brief practical description of the system as an introduction to study transient events. The reader can refer to [31] for more details. The apparatus construction retained many of the features described by previous related investigators [16,17]. The working medium is air ($Pr \approx 0.71$) and the modified Rayleigh number Ra^* is changed by the heat rate q' and the cylinder diameter D.

A tungsten wire was mounted in an insulated test chamber. Tungsten was chosen because it has low thermal emission and high thermal conductivity. Wires of 0.200 ± 0.005 and 0.400 ± 0.005 mm were used in the experiments. Diameters were determined by a precision micrometer. The test wire was secured between terminal posts 28.0 cm apart and carefully aligned with the optical axis. The aspect ratios (length/diameter) were respectively 1400 and 700, in order to reduce end effects.

The horizontal cylinder was heated by flowing an electrical current through it. The time, at which current was applied, was marked by the firing of a led. An infrared camera (not shown in Fig. 1) was used to record the surface temperature of the wire. The wire itself is

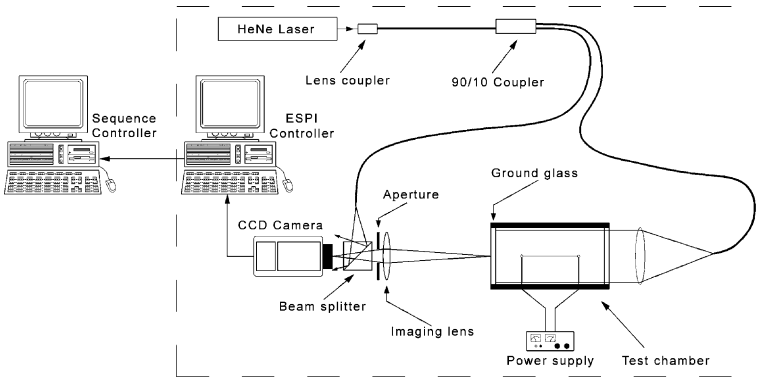

Fig. 1. Experimental setup.

both a heater and a thermometer, therefore its mean temperature can be determined from the electrical resistance. We used an infrared camera to add the system the capability of studying different transients, such those, for instance, in electronics components. The infrared setup was calibrated taking into account the procedure suggested by Maranzana et al. [14] to minimize the effect of ambient radiation and the information obtained from the electrical resistance of the wire. The uncertainty in the reconstructed temperature was about ±4 °C. The effects of this error will be discussed in detail in Section 3.

The system within the dotted box in Fig. 1 is a standard ESPI arrangement [31]. The basic principle of ESPI is the recording of a holographic speckle pattern sequence on the photosensor of a TV camera. Holographic speckle patterns contain information about both amplitude and phase of the wave. They are obtained when the scattered wavefront emanating from the surface is recorded simultaneously with a reference wavefront.

The interferometer consists of an optical head and a personal computer (ESPI controller). Coherent light coming from a He–Ne laser (power $P = 35$ mW, wavelength $\lambda = 632.8$ nm) is coupled by a gradient index rod microlens to a single mode fibre. A fibre optics 10/90 directional coupler (Fibercore SC-633-10-0.5) splits the light beam into two: the object beam, which travels through the test chamber, and the reference beam. A beamsplitter cube, placed between the photo sensor and the imaging lens, couples the light diffused by the ground glass to the reference beam, thus producing a holographic speckle pattern on the CCD. We used a standard B&W camera (Sony XC-73) with a $1/3''$ CCD and 768×494 pixels.

The pattern resulting from this cross-interference is recorded by the camera, converted to a video signal, sampled and stored in a digital frame memory. The frame grabber (Coreco Oculus 300) is a standard video system, with a 8 bit analogue-digital converter and a resolution of 512×512 pixels. It is equipped with four memories (frame buffers) where the images are temporarily stored. This frame grabber is also equipped with an on-board processor; therefore, the frame grabber is suitable to perform digital subtraction in quasi-real time, that means during the frame refresh.

The final ESPI interferogram is generated arithmetically by subtracting two digitized speckle patterns. The subtraction process ensures a significant reduction of the fixed noise (optical noise). During the experiments, the incoming patterns can be taken continuously, digitized and subtracted from the reference state. The reference state was obtained leaving the system undisturbed for a few hours before each run, so that the fluid becomes quiescent and isothermal with the wire.

Note that each processed video frame can be considered a recorded and reconstructed hologram. Consequently, 25 holograms (by the European TV standard) are presented on the TV monitor each second. Thanks to this high repetition rate, combined with the relatively short exposure time of 40 ms (European TV standard), the technique is not affected by the instabilities that would destroy most conventional interferometric images. Therefore, it can be used also in laboratories non-specifically devoted to optical diagnostics.

It is then clear that, from an operational point of view, ESPI is faster and simpler to use than conventional holography or interferometry. Furthermore, it is suitable for in situ routine measurements.

The resulting fringes, displayed in quasi-real time on a TV monitor, are similar in appearance to conventional holographic fringes, but they are very noisy, due to the larger speckle size. For this reason, ESPI fringes should be electronically treated for noise removal and contrast enhancement. Applications requiring only a qualitative interpretation, can be easily followed directly on the TV monitor.

If L is the cylinder length, the phase perturbation experienced by the beam, due to a temperature change ΔT, can be written as

$$\Delta\varphi(x,y) = \frac{2\pi L}{\lambda}\left(\frac{\mathrm{d}n}{\mathrm{d}T}\right)\Delta T(x,y), \tag{5}$$

the value of the derivative of the refractive index $(\mathrm{d}n/\mathrm{d}T)$ can be found in literature [23,27].

If a squared difference is performed between two intensity speckle patterns, recorded at different times, the resulting pattern can be described as [31]

$$I(x,y) = 8I_o(x,y)I_r(x,y)\sin^2\left[\vartheta(x,y) + \frac{\Delta\varphi(x,y)}{2}\right] \times \{1 - \cos[\Delta\varphi(x,y)]\}, \tag{6}$$

where $I_o(x,y)$ and $I_r(x,y)$ are the object and reference beam intensities and $\Delta\varphi(x,y)$ contains the desired information about temperature variation. The multiplicative noise interference term $\sin^2[\vartheta(x,y) + \Delta\varphi(x,y)/2]$, can be reduced taking an average operation over many speckles. Assuming that the following relation holds

$$\left\langle \sin^2\left[\vartheta(x,y) + \frac{\Delta\varphi(x,y)}{2}\right]\right\rangle = \frac{1}{2}, \tag{7}$$

where the angle brackets denote the averaging operation, Eq. (6) can be rewritten as

$$I(x,y) = 4I_o(x,y)I_r(x,y)\{1 - \cos[\Delta\varphi(x,y)]\}. \tag{8}$$

By comparing Eqs. (5) and (8), it is confirmed that isophase lines, where the term in braces parentheses in Eq. (8) is null, are also isothermal lines. Eq. (8) is equivalent to the classical interferometry equation. It describes perfect correlation fringes without speckles. In practice, due to speckle decorrelation, fringe visibility is always <1. Fringes visualization on a monitor is sufficient for qualitative investigation. For quantitative evaluation, the temperature information has to be numerically extracted [23,38].

So far, we have discussed a standard ESPI system (the arrangement within the dotted box in Fig. 1) to investigate heat and mass transfer processes. Such a system can be easily used to study transient processes, thanks to a full exploitation of the frame grabber features. The frame grabber is capable to construct ESPI interferograms (by digital subtraction) in quasi-real time. If the video output is connected to a second computer (sequence controller in Fig. 1), we obtain a digital sequence of interferograms, recorded at a speed of 25 frames/s. In other words, the time interval between each image of the sequence is 0.04 s. This time resolution appears well suited to investigate relatively slow processes, as those discussed in this paper. A time resolution in the range of μs requires pulsed lasers and/or high-speed cameras [36,37,39,40].

In summary, ESPI is an interesting tool to study heat and mass transfer phenomena due to its relatively low cost (if only standard lasers, cameras and frame grabbers are used) and its capability to provide full-field, interferometric-like images while relaxing a number of operational practical difficulties inherent in interferometry and holographic interferometry [23,27]. Main limitations are image noise (speckle noise) and spatial resolution of the CCD camera. In fact, individual speckles must be resolved by the TV camera to optimize both the performance and the fringe visibility [31]. With a typical pixel size of ~10 μm, an f-number of 16 is needed. On the other hand, relatively large f-numbers will give large speckles, which affect system performances in several ways. Firstly, the light intensity in the image is reduced, thus reducing the signal dynamic unless higher power lasers and/or higher sensitivity cameras are used (with a much higher cost). A second consequence is that the speckles are clearly seen in the image, reducing fringe quality and acting as a noise.

A further limitation is due to the TV camera spatial resolution. In fact, a minimum of 20 pixels is required to resolve a fringe. If we use a standard camera with 512×512 pixels, a maximum of about 25 equally spaced fringes can be resolved. In heat transfer problems, the fringes density depends on the temperature gradient: spacing is large in regions of small gradient and small in regions of high temperature gradient. Therefore, a suitable inspection area must be chosen.

3. Experimental results and discussion

For both test wires, experimental runs were performed according to the following procedure:

1. Positioning of the wire under test and waiting for the thermal equilibrium between wire and ambient air.
2. Recording of the first "undisturbed" image (i.e. with the wire in thermal equilibrium with air) in the ESPI controller computer.
3. Construction of ESPI interferograms by continuously subtracting (at a speed of 25 frames/s) a freshly captured image from the first image. At this stage (still undisturbed) no fringes appear on the monitor.
4. Beginning of recording ESPI interferograms sequence in the sequence controller computer. The duration of each sequence was suited to transient duration by separate experimental runs.
5. Heating of the wire by a given input of electrical power. The lighting of a led in the field of view marked the zero of time for the experiment. For both wires, test were conducted by imposing three constant linear heat fluxes of 10.7, 14.3, 17.8 W/m.
6. Analysis of each ESPI sequence frame-by-frame and, within a frame, pixel-by-pixel, in order to obtain the time at which observable convection begins.

The ambient air temperature was measured by two thermocouples positioned within the test chamber. As a

check rule, they must detect the same temperature at beginning and end of the transient. All the fluid properties were evaluated at film temperature $T_f = (T_w + T_\infty)/2$.

First, attention is devoted to flow visualization and then to the determination of time delay. The results of Vest and Lawson [16] and Parsons and Mulligan [17] represent the convenient context within which to discuss the present experiment.

3.1. Visualization of the temperature field

In this section we will adopt a very visual approach; as far as we are concerned, very few visualizations of transient convection on circular cylinders in air have been published. Fig. 2 shows a typical "standard" sequence of Dynamic-ESPI interferograms, recorded at different times t after application of current to the wire. Cylinder diameter was 0.200 ± 0.005 mm while the heating rate q' was 10.7 W/m.

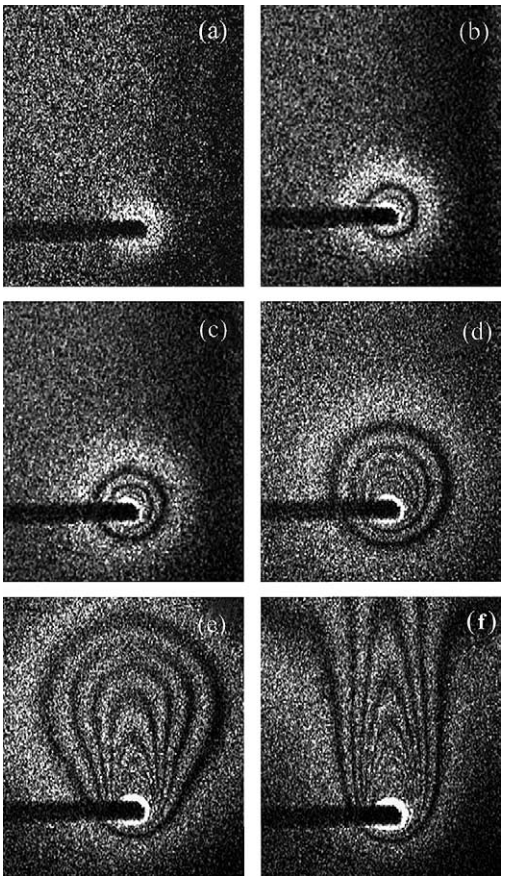

Fig. 2. Onset and development of convection from a tungsten wire (28.0 cm long, 0.200 ± 0.005 mm diameter, $q' = 10.7$ W/m). (a) 0.12 s; (b) 0.36 s; (c) 0.52 s; (d) 0.68 s; (e) 1.1 s; (f) 1.56 s. Each image has a time indetermination of ±0.04 s.

Initially, the isotherms are concentric circles, indicating pure conduction (Fig. 2(a) and (b)). This initial conductive transfer, characterized by concentric circled isotherms, was observed experimentally by Ostroumov [15] and Vest and Lawson [16]. Parsons and Mulligan [17] deduced the existence of a distinct limit of pure conduction from the transient decay of the Nusselt number vs. the Fourier number: an abrupt deviation from the pure conduction trend marked the limit of pure conduction. At increasing times, the isotherms become asymmetrical, as those above the wire are convected upward (Fig. 2(c)). At greater times, convective effects become important (Fig. 2(d) and (e)). The temperature difference between each fringe is about 3 °C. Note that some fringes are not resolved because of speckle noise, diffraction effects and poor spatial resolution. The interferograms show how the upward transport accelerates towards a steady state (Fig. 2(f)). The behavior of the other cylinder (0.400 ± 0.005 mm in diameter) is qualitatively the same.

Further insight into the process can be obtained. Fig. 3 shows the temperature field around the 0.2 mm cylinder, at time 0.92 s after the application of current, for three heating rates: 10.7, 14.3 and 17.8 W/m. A qualitative comparison of the patterns confirms that beginning of observable convection (time delay) is inversely proportional to the heating rate, see Eq. (1). The temperature pattern in Fig. 3(a) ($q' = 10.7$ W/m, $t = 0.92$ s) shows a certain lack of circular symmetry. At the same time, the wires heated at 14.3 W/m and at 17.8 W/m are well ahead towards the steady state, exhibiting the familiar mushroom-shaped plume (Fig. 3(b) and (c)).

The effect of the cylinder diameter can also be qualitatively investigated. Fig. 4 compares the temperature field around the two wires at the same times using two different heating rates. In particular, Fig. 4(a) and (b) are taken after 0.84 ± 0.04 s with heating rate 10.7 W/m, while Fig. 4(c) and (d) are taken after 1.04 ± 0.04 s with heating rate 14.3 W/m. The interferograms related to the 0.4 mm wire (Fig. 4(b) and (d)) show a clear delay with respect to the interferograms of the 0.2 mm wire (Fig. 4(a) and (c)). These results seem to suggest that the time, at which observable convection begins, increases with the wire diameter.

3.2. Time delay

The sequences of Dynamic-ESPI interferograms, recorded at different times t after application of current to the wire, can also be used to determine the critical times for onset of convection. In this paper we chose the same approach of Vest and Lawson [16]: the onset of convection is denoted by a lack of symmetry in the outermost isotherm. The sequences are digitally stored, therefore they can be analyzed frame-by-frame and pixel-by-pixel. The time indetermination (connected

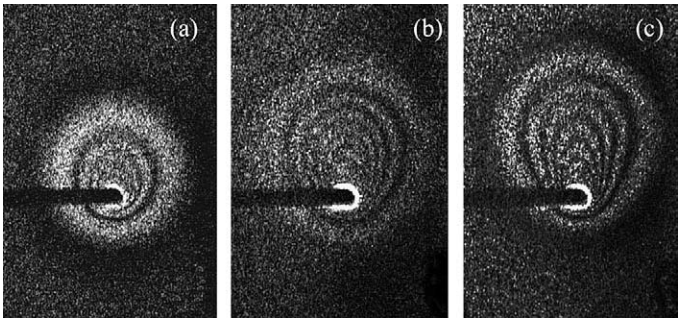

Fig. 3. Temperature patterns from a tungsten wire (28.0 cm long, 0.200 ± 0.005 mm diameter, $t = 0.92 \pm 0.04$ s). (a) $q' = 10.7$ W/m; (b) $q' = 14.3$ W/m; (c) $q' = 17.8$ W/m.

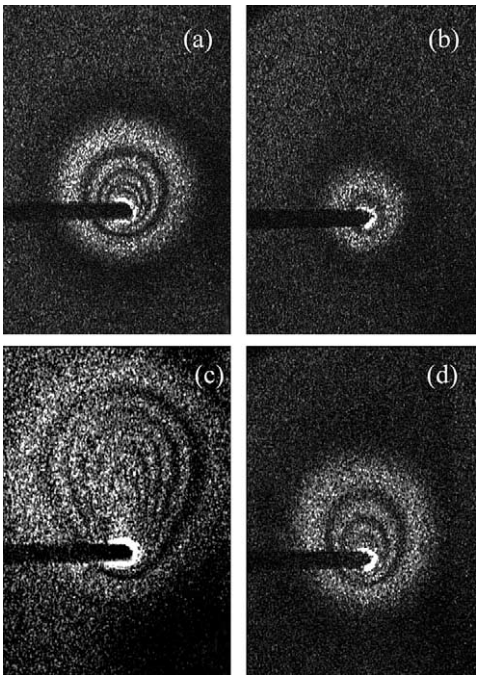

Fig. 4. Temperature patterns from a tungsten wire (28.0 cm long). Heating rate $q' = 10.7$ W/m, $t = 0.84 \pm 0.04$ s. (a) Wire diameter 0.200 ± 0.005 mm. (b) Wire diameter 0.400 ± 0.005 mm. Heating rate $q' = 14.3$ W/m, $t = 1.04 \pm 0.04$ s. (c) Wire diameter 0.200 ± 0.005. (d) Wire diameter 0.400 ± 0.005 mm.

with the frame sampling) is $1/25 = 0.04$ s. Values of Ra^* ranging from 0.069 to 0.769 were used.

The modified Rayleigh number Ra^* does not depend directly on the temperature difference $(T_w - T_\infty)$, therefore the uncertainties in the related measurements have an influence on Ra^* only through the variations of the fluid properties. The error on T_f is ±2 °C, which implies an error on fluid properties within ±0.7%. This was considered negligible and, consequently, uncertainty in Ra^* is due mainly to uncertainty in q' and d. Taking into account the accurate evaluation of the input power and the error on the cylinder diameter, tolerances in Ra^* were reduced to ±7%.

The uncertainty in time delay τ_D is strictly related to the accuracy of delay determination t^* and of the cylinder diameter d. By a standard propagation of errors the uncertainty in τ_D ranges from 20% (for the 0.2 mm wire with $q' = 17.8$ W/m) to 9% (for the 0.4 mm wire with $q' = 10.7$ W/m). In the following plots, the experimental error bars are omitted because they fall within the diamond markers.

Fig. 5 shows the results of this experiment compared with previous data for air, water and alcohol. The two lines are the analytical correlation of Vest and Lawson, Eq. (2), and the first regression line of Parsons and Mulligan, Eq. (3).

Our data follow the general trend of equation A–A and B–B, however they slightly fall above the two lines. Vest and Lawson observed a similar behavior in their data with respect to equation A–A.

The results of this experiment show a deviation within 30%. In particular, experimental results from the 0.2 mm wire fall within 15% from both lines, while results from the 0.4 mm wire are within 30%.

Of particular interest is a comparison of the air data only. Fig. 6 shows the existing data for air compared with the second correlation of Parsons and Mulligan Eq. (4). In this case, the deviation of the present results are within 9% for the 0.2 mm wire and within 18% for the 0.4 mm wire.

Finally, an attempt was made to better describe the wire behavior by re-correlating the air data. We used our own data for 0.2 and 0.4 mm wires, Vest and Lawson's data for a 0.2 mm wire and Parsons and Mulligan's results for a 0.127 mm wire. The best fit regression line (least squares) through these data can be written as

$$\tau_D = 229.3(Ra^*)^{-0.53}. \quad (9)$$

Fig. 7 shows the results compared to Eq. (9). Parsons and Mulligan data for a 0.030 mm wire (black filled

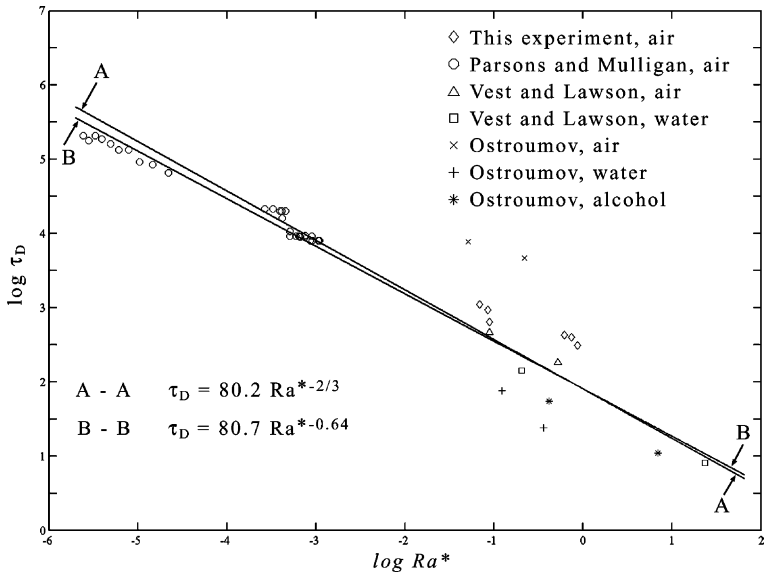

Fig. 5. Time delay τ_D as a function of modified Rayleigh number Ra^*: comparison of experimental data with correlations based on thermal stability criteria.

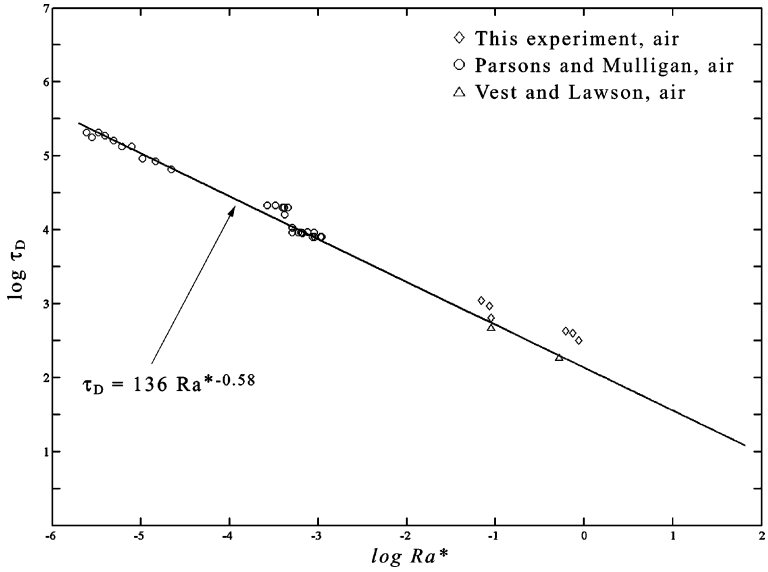

Fig. 6. Time delay τ_D as a function of modified Rayleigh number Ra^*: air data only.

circles) have been excluded from the correlation and then used as check data. The present results now fall within ±4% (0.2 mm wire) and ±7% (0.4 mm wire). On the other hand, "small wires" (black filled circles in Fig. 7) still correlate successfully, within ±2%.

The present experiment confirms that the standard correlation for delay time, Eq. (2), can lead to consistent underestimation in air. Better accuracy can be obtained using the correlation of Parsons and Mulligan for air, Eq. (4). In any case, our results outline the accuracy that can be obtained extending the existing correlations to wires with diameter of 0.4 mm. The delay time for these diameters can be more accurately predicted using Eq. (9).

As a final remark, an examination of the raw data (see Table 1) shows that time, at which observable convection begins, increases with the diameter (see also the previous section). This behavior is not acquainted in the ideal model. In fact, taking into account Eq. (2) and

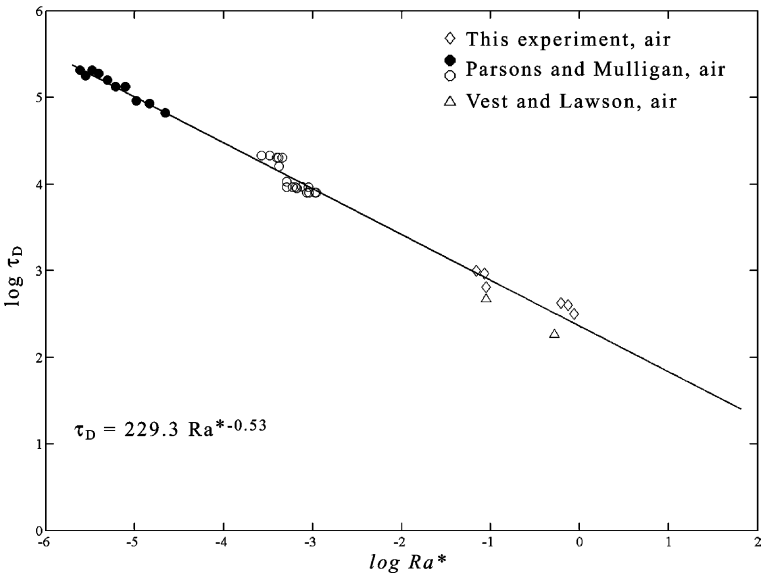

Fig. 7. Comparison of air data for τ_D with the proposed correlation. Results from the smallest wire (black filled circles) were excluded from the correlation and then used as check data.

Table 1
Experimental results

d (mm)	q' (W/m)	ΔT (K)	T_f (K)	Time of onset (s)
0.2	10.7	52	319	0.40 ± 0.04
0.2	14.3	65	326	0.36 ± 0.04
0.2	17.8	85	336	0.24 ± 0.04
0.4	10.7	40	313	0.72 ± 0.04
0.4	14.3	55	321	0.64 ± 0.04
0.4	17.8	75	331	0.48 ± 0.04

the definition of τ_D, the time t at which convection begins does not depend on the wire diameter. This is probably due to the neglecting of the wire capacity, which practically acts as a thermal inertia. This explains why correlations for air, Eqs. (4) and (9) exhibit exponents which, more or less significantly, differ from −2/3.

4. Conclusions

The purpose of this work was to visualize temperature patterns in air and to provide more quantitative data for the onset of free convection from a suddenly heated horizontal wire. A technique, called Dynamic-ESPI, was proposed to investigate transient event in heat transfer. This technique has the sensitivity of holographic interferometry but has less stringent stability requirements. Furthermore, it allows to operate in daylight as well by using a simple interference filter. The major features are the ability to present correlation real time fringes directly on a TV monitor and a full digital data elaboration. ESPI interferograms are inherently very noisy. This is the major drawback.

It is believed that future trends in ESPI will employ large area CCDs, TV-cameras with higher sensitivity and dynamic range and more powerful image processing software. Their wide availability at a relatively low cost should alleviate the present disadvantages.

In order to investigate the flow and to evaluate the time at which observable convection begins, experiments were performed on tungsten wires of two diameters, 0.2 and 0.4 mm, using three different heating rates, 10.7, 14.3 and 17.8 W/m. The heat-rate-based Rayleigh number, Ra^*, ranges from 0.069 to 0.67.

The conclusions can be summarized as follows:

1. Dynamic-ESPI is a relatively low cost technique, which is suitable to investigate relatively slow transient processes, as those described in this paper. The time resolution is 1/25 s.
2. As far as we are concerned, very few full-field experimental measurements are available in literature about transient convection from a horizontal cylinder in air. Therefore, Dynamic-ESPI was used to perform qualitative and quantitative investigation.
3. Qualitative flow visualization clearly confirmed the existence of a convective delay and suggested that this delay increases with the diameter.
4. Time delay was determined using the visual criteria of Vest and Lawson. Experimental results are in good agreement with Vest and Lawson and Parsons and Mulligan correlations. Deviation ranges from 9% to 30%.

5. A new correlation was given, re-correlating our data with Vest and Lawson's results and the delay times of Parsons and Mulligan's larger diameter (0.127 mm). In this case, deviation ranges from 4% to 7%. This correlation is valid also for 0.4 mm wires, a diameter not covered by previous experiments.

Acknowledgements

The authors wish to thank J.C. Mulligan for the useful information provided.

References

[1] A. Bejan, Convection Heat Transfer, second ed., Wiley, New York, 1995.
[2] A.J. Ede, Advances in free convection, in: T.F. Irvine, J.P. Harnett (Eds.), Advances in Heat Transfer, vol. 4, Academic Press, New York, 1968, pp. 1–64.
[3] S. Kakaç, W. Aung, R. Viskanta (Eds.), Natural Convection, Hemisphere Publishing, New York, 1985.
[4] W.M. Kays, M.E. Crawford, Convective Heat and Mass Transfer, third ed., McGraw-Hill, New York, 1993.
[5] G.T. Raithby, K.G.T. Holland, Natural convection, in: W.M. Rohsenow, J.P. Hartnett, Y.I. Cho (Eds.), Handbook of Heat Transfer, third ed., McGraw-Hill, New York, 1998 (chapter 4).
[6] V.T. Morgan, The overall convective heat transfer from smooth circular cylinders, in: T.F. Irvine, J.P. Harnett (Eds.), Advances in Heat Transfer, vol. 11, Academic Press, New York, 1975, pp. 199–264.
[7] T.H. Kuehn, R.J. Goldstein, Numerical solution to the Navier–Stokes equations for laminar natural convection about a horizontal isothermal circular cylinder, Int. J. Heat Mass Transfer 23 (1980) 971–979.
[8] S. Nakai, T. Okazaki, Heat transfer from a horizontal circular wire at small Reynolds and Grashof numbers—1. Pure convection, Int. J. Heat Mass Transfer 18 (1975) 387–396.
[9] S.W. Churchill, H.H.S. Chu, Correlating equations for laminar and turbulent free convection from a horizontal cylinder, Int. J. Heat Mass Transfer 18 (1975) 1049–1053.
[10] L. Crescentini, G. Fiocco, Interferometric investigations of convection around cylinders at small Grashof numbers, Appl. Optics 29 (1990) 1490–1495.
[11] H. Koizumi, I. Hosokawa, Chaotic behavior and heat transfer performanceof the natural convection around a hot horizontal cylinder affected by a flat ceiling, Int. J. Heat Mass Transfer 39 (1996) 1081–1091.
[12] K. Kitamura, F. Kami-iwa, T. Misumi, Heat transfer and fluid flow of natural convection around large horizontal cylinders, Int. J. Heat Mass Transfer 42 (1999) 4093–4106.
[13] R.J. Goldstein, R.J. Volino, Onset and development of natural convection above a suddenly heated horizontal surface, ASME J. Heat Transfer 117 (1995) 808–821.
[14] G. Maranzana, S. Didierjean, B. Rémy, D. Maillet, Experimental estimation of the transient free convection heat transfer coefficient on a vertical flat plate in air, Int. J. Heat Mass Transfer 45 (2002) 3413–3427.
[15] G.A. Ostroumov, Unsteady heat convection near a horizontal cylinder, Sov. Tech. Phys. 1 (1956) 2627–2641.
[16] C.M. Vest, M.L. Lawson, Onset of convection near a suddenly heated horizontal wire, Int. J. Heat Mass Transfer 15 (1972) 1281–1283.
[17] J.R. Parsons, J.C. Mulligan, Transient free convection from a suddenly heated horizontal wire, ASME J. Heat Transfer 100 (1978) 423–428.
[18] J.H. Blackwell, A transient-flow method for determination of thermal constants of insulating materials in bulk, J. Appl. Phys. 25 (1954) 137–144.
[19] H.S. Carslaw, J.C. Jaeger, Conduction of Heat in Solids, second ed., Oxford University Press, London, 1959, pp. 342–345.
[20] A.R. Pellew, R.V. Southwell, On maintained convective motion in a fluid heated from below, Proc. Roy. Soc. A 176 (1940) 312–343.
[21] T. Saitoh, T. Sajiki, K. Maruhara, Bench mark solutions to natural convection heat transfer problem around a horizontal circular cylinder, Int. J. Heat Mass Transfer 36 (1993) 1251–1259.
[22] A. Linan, V.N. Kurdyumov, Laminar free convection induced by a line heat source, and heat transfer from wires at small Grashof numbers, J. Fluid Mech. 362 (1998) 199–227.
[23] W. Hauf, U. Grigull, Optical methods in heat transfer, in: T.F. Irvine, J.P. Harnett (Eds.), Advances in Heat Transfer, vol. 6, Academic Press, New York, 1970, pp. 133–362.
[24] F. Mayinger (Ed.), Optical Measurements, Springer-Verlag, Berlin, 1994.
[25] R.J. Goldstein, T.H. Kuehn, Optical systems for flow measurement: shadowgraph schlieren and interferometric techniques, in: R.J. Goldstein (Ed.), Fluid Mechanics Measurements, second ed, Taylor & Francis, Washington, 1996, pp. 451–508.
[26] W. Merzkirch, Flow Visualization, second ed., Academic Press, Orlando, 1987.
[27] C.M. Vest, Holographic Interferometry, Wiley, New York, 1979.
[28] N.A. Fomin, Speckle Photography for Fluid Mechanics Measurements, Springer-Verlag, Berlin, 1998.
[29] G.S. Settles, Schlieren and Shadowgraph Techniques, Springer-Verlag, Berlin, 2001.
[30] S.V. Garimella, Flow visualization methods and their application in electronic systems, in: K. Azar (Ed.), Thermal Measurements in Electronics Cooling, CRC Press, New York, 1997, pp. 349–385.
[31] P.K. Rastogi (Ed.), Digital Speckle Pattern Interferometry and Related Techniques, Wiley, Chicester, 2001.
[32] D. Paoletti, G. Schirripa Spagnolo, V. Bagini, M. Santarsiero, A new method for measuring the diffusivity of liquid binary mixtures using DSPI, Pure and Applied Optics 2 (1993) 489–498.
[33] G. Schirripa Spagnolo, D. Paoletti, D. Ambrosini, V. Bagini, M. Santarsiero, Fourier transform evaluation of digital interferograms for diffusivity measurements, Pure Appl. Optics 3 (1994) 249–253.
[34] G. Schirripa Spagnolo, D. Ambrosini, A. Ponticiello, D. Paoletti, Temperature measurement in laminar free con-

vection using electro-optic holography, J. Phys. III (Fr.) 7 (1997) 1893–1898.
[35] See the ESPI online bibliography at the Home Page of Optical Methods in Heat and Mass Transfer: http://dau.ing.univaq.it/omhat.
[36] A.J. Moore, J.D.C. Jones, J.D.R. Valera, Dynamic measurements, in: P.K. Rastogi (Ed.), Digital Speckle Pattern Interferometry and Related Techniques, Wiley, Chicester, 2001, pp. 225–288.
[37] M.A. Ahmadshahi, S. Krishnaswamy, S. Nemat-Nasser, Dynamic holographic electronic speckle pattern interferometry, ASME J. Appl. Mech. 60 (1993) 866–874.
[38] D.W. Robinson, G.T. Reid (Eds.), Interferogram Analysis, Institute of Physics, Bristol, 1993.
[39] G. Pedrini, H.J. Tiziani, Double-pulse electronic speckle interferometry for vibration analysis, Appl. Opt. 33 (1994) 7857–7863.
[40] A. Fernández, A.J. Moore, C. Pérez-López, A.F. Doval, J. Blanco-García, Study of transient deformations with pulsed TV holography: application to crack detection, Appl. Opt. 36 (1997) 2058–2065.